# An Intersubunit Disulfide Bond Prevents in Vitro Aggregation of a Superoxide Dismutase-1 Mutant Linked to Familial Amytrophic Lateral Sclerosis

**ARTICLE** *in* BIOCHEMISTRY · JUNE 2004

Impact Factor: 3.02 · DOI: 10.1021/bi030246r · Source: PubMed



**6 AUTHORS**, INCLUDING:

Soumya S Ray
Brigham and Women's Hospital
**23** PUBLICATIONS **596** CITATIONS

SEE PROFILE

Richard J Nowak
Yale University
**19** PUBLICATIONS **1,314** CITATIONS

SEE PROFILE

# An Intersubunit Disulfide Bond Prevents in Vitro Aggregation of a Superoxide Dismutase-1 Mutant Linked to Familial Amytrophic Lateral Sclerosis†

Soumya S. Ray,*,‡,§ Richard J. Nowak,‡,§ Konstantin Strokovich,⊥ Robert H. Brown, Jr.,‡,|| Thomas Walz,⊥ and Peter T. Lansbury, Jr.*,‡,§

*Harvard Center for Neurodegeneration and Repair and Department of Neurology, Harvard Medical School, Boston, Massachusetts 02115, Center for Neurologic Diseases, Brigham and Women's Hospital, 65 Landsdowne Street, Cambridge, Massachusetts 02139, Department of Cell Biology, Harvard Medical School, Boston, Massachusetts 02115, and Center for Aging, Genetics and Neurodegeneration, Massachusetts General Hospital, Charlestown, Massachusetts 02129*

*Received November 26, 2003; Revised Manuscript Received March 4, 2004*

ABSTRACT: Familial amyotrophic lateral sclerosis (FALS) is linked to over 90 point mutations in superoxide dismutase-1 (SOD1), a dimeric metalloenzyme. The postmortem FALS brain is characterized by SOD1 inclusions in the motor neurons of regions in which neuronal loss is most significant. These findings, together with animal modeling studies, suggest that aggregation of mutant SOD1 produces a pathogenic species. We demonstrate here that a mutant form of SOD1 (A4V) that is linked to a particularly aggressive form of FALS aggregates in vitro, while wild-type SOD1 (WT) is stable. Some A4V aggregates resemble amyloid pores formed by other disease-associated proteins. The WT dimer is significantly more stable than the A4V dimer, suggesting that dimer dissociation may be the required first step of aggregation. To test this hypothesis, an intersubunit disulfide bond between symmetry-related residues at the A4V dimer interface was introduced. The resultant disulfide bond (V148C−V148C′) eliminated the concentration-dependent loss of enzymatic activity of A4V, stabilized the A4V dimer, and completely abolished aggregation. A drug-like molecule that could stabilize the A4V dimer could slow the onset and progression of FALS.

Amyotrophic lateral sclerosis (ALS, Lou Gehrig's disease) is a relatively common adult-onset neurodegenerative disease, having a worldwide prevalence of ca. 5 per 100000 (*1*). ALS is characterized by the selective degeneration of spinal cord motor neurons (*2*), leading to rapid and progressive atrophy of skeletal muscles. Death typically occurs by asphyxia, almost always within 5 years of diagnosis. There is no effective therapy.

Approximately 10% of ALS cases are autosomal-dominantly inherited (FALS)[1]. Of these, ca. 20% involve missense mutations in the gene encoding superoxide dismutase-1 (SOD1), a housekeeping metalloprotein responsible for dismutation of superoxide. Over 90 FALS-linked SOD1 mutations have been characterized (*3*−*6*). Animal modeling studies indicate that the pathogenicity of the SOD1 mutations does not involve loss of its normal function, but rather the gain of a toxic function (*7*−*10*). The mechanism of pathogenicity is unknown. One hypothesis holds that mutant forms of SOD1 have abnormal and toxic enzymatic activity (*11*).

Degenerating populations of motor neurons in postmortem FALS brain are characterized by abnormal proteinaceous cytoplasmic inclusions. These inclusions contain mutant SOD1. Since several FALS mutations affect the stability or unfolding of SOD1 or both (*12*−*14*), it has been suggested that aggregation of mutant SOD1 produces a pathogenic species. However, the identity of the pathogenic aggregate and the mechanism linking aggregation and neurotoxicity remain elusive (*15*). Although fibrillar substructure has not been conclusively detected in FALS inclusions, parallels between FALS and other familial neurodegenerative diseases suggest that the process of SOD1 aggregation, if not the product, may resemble aggregation of the proteins linked to those diseases (*16*).

The FALS mutations are distributed throughout the SOD1 primary and tertiary structures. Some, but not all of the mutations are known to affect SOD1 stability (*11*, *17*−*23*). Others affect metal binding or enzymatic activity or both (*12*, *24*−*26*). We demonstrate here that the FALS mutant A4V, which is linked to a common early onset and rapidly progressing (typically 1 year between diagnosis and death (*27*)) form of FALS, spontaneously aggregates in vitro under conditions at which the WT dimer is stable. At low protein concentrations A4V, but not WT, populates a monomeric form. To determine whether the reduced stability of the A4V dimer was wholly or partly responsible for its rapid aggrega-

† This work was supported by the National Institutes of Health (Grant AG08476 to P.L.). The molecular electron microscopy facility at Harvard Medical School was established by a generous donation from the Giovanni Armenise Harvard Center for Structural Biology and is maintained by funds from NIH Grant GM62580.

* To whom correspondence should be addressed. E-mail addresses: sray@rics.bwh.harvard.edu; plansbury@rics.bwh.harvard.edu.

‡ Harvard Center for Neurodegeneration and Repair and Department of Neurology, Harvard Medical School.

§ Brigham and Women's Hospital.

⊥ Department of Cell Biology, Harvard Medical School.

|| Massachusetts General Hospital.

[1] Abbreviations: A4V, the FALS-linked SOD1 point mutant alanine 4 to valine; EM, electron microscopy; FALS, familial amyotrophic lateral sclerosis; SOD1, human superoxide dismutase-type 1; Tg, transgenic; WT, wild-type SOD1.

10.1021/bi030246r CCC: $27.50 
Published on Web 04/06/2004

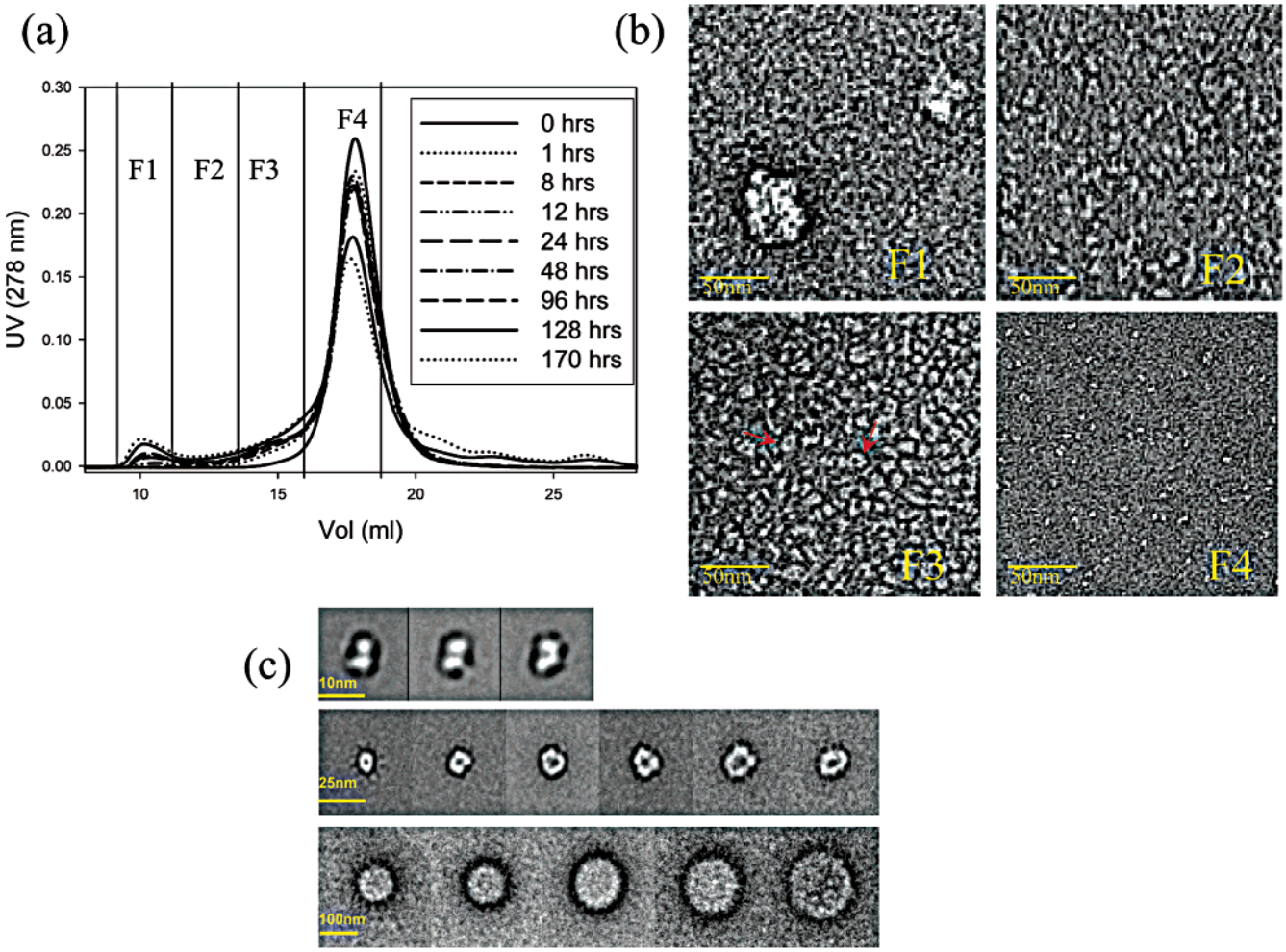


FIGURE 1: (a) Aggregation of A4V followed by size-exclusion chromatography (Superdex 200) as a function of time at 37 °C. The appearance of aggregates corresponded with the loss of dimer. (b) Negative-staining electron microscopy of A4V aggregate fractions collected after 175 h. The vertical bars drawn on the chromatography profile (panel a) indicate each fraction. (c) Averaged EM images show three morphological types: dimers (top panels), pore-like structures (middle panels), and large spherical aggregates (bottom panels).

tion, we engineered an intersubunit disulfide bridge across the A4V dimer interface to produce an A4V/V148C covalent dimer that could not monomerize. This mutant SOD1 did not aggregate in vitro, suggesting a novel therapeutic strategy against FALS.

## MATERIALS AND METHODS

*Expression and Purification of Human SOD1 Variants (WT, A4V, and A4V/V148C).* Genes encoding human SOD1, WT and A4V, were cloned by a PCR strategy into pGex6P1 (Amersham) using the *Bam*H1 and *Xho*1 restriction sites of the vector. SOD1 was expressed as a glutathione-S-transferase (GST) fusion in the Rosetta *Escherichia coli* strain (Novagen). During IPTG induction, 200 $\mu$M copper chloride and zinc chloride were added to the growth media without any apparent toxicity. Recombinant proteins were purified to homogeneity with GST−agarose affinity matrix (Pharmacia) and anion-exchange chromatographies. Following proteolytic cleavage of the affinity tag with PreCission protease (Pharmacia) (cut site, $NH_2$−LEVLFQLP−COOH) and removal of the tag (three ($NH_2$−GPL−) remained at the N-terminus of the protein, but this had no effect on A4V behavior as compared to A4V expressed in insect cells, which was kindly provided to us by Larry Hayward), the molecular masses of WT, A4V, V148C, and A4V/V148C were determined by matrix-assisted laser desorption ionization (MALDI) mass spectrometry (under oxidizing conditions, the dimeric forms of A4V/V148C (32 775 Da) and V148C (32 721 Da) were characterized). The purity of each protein was greater than 99%, as judged by SDS−PAGE.

*Measurement of SOD1 Enzymatic Activity.* The superoxide dismutase activity of WT and A4V was measured by a coupled enzyme assay using xanthine oxidase to generate superoxide. SOD1 activity was measured colorimetrically with (2,3-bis(2-methoxy-4-nitro-5-sulfophenyl)-2*H*-tetrazolium-5-carboxanilide) (*28*).

*Monitoring SOD1 Aggregation by Gel Filtration and Light Scattering.* Dimeric SOD1 was purified on a Superdex 75 (16/60) gel-filtration column (Pharmacia) to produce starting material for each aggregation experiment. Incubation was performed at 37 °C, and aliquots were periodically removed and analyzed by gel filtration on a Superdex 200 (3.2/30) gel-filtration column (Pharmacia). All chromatography was performed in TBS (20 mM Tris, 150 mM NaCl), pH 7.4, on a Waters 2690 Alliance HPLC or Agilent 1100 series HPLC and monitored at 276 nm. After 80 h, three fractions (Figure 1) were collected and analyzed by electron microscopy. An online multiangle light scattering (MALS) detector (DAWN EOS, Wyatt Technology, Santa Barbara, CA) and differential refractive index (DRI) detector (Optilab DRI, Wyatt Tech-

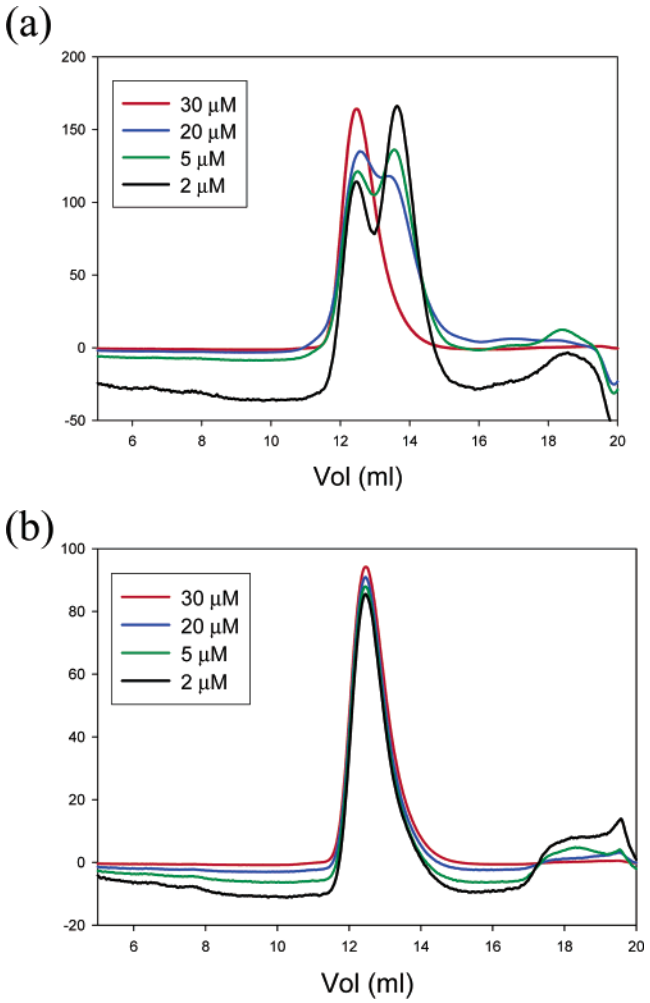


FIGURE 2: (a) Size-exclusion chromatography (Superdex 75) profile for A4V as a function of protein concentration followed over a concentration range of 2−30 $\mu$M. The peak that elutes at ca. 14 mL and is populated at low concentration was determined to be monomeric SOD from light scattering studies. (b) WT was completely dimeric over the same concentration range.

nology) setup was used to measure the light scattered as a function of angle and absolute protein concentration of fractions eluting from the size-exclusion chromatography column. The Rayleigh−Gans−Debye approximation was used in the Astra software (Wyatt Technology) to estimate molar mass. Data were fit using a first-order polynomial. For the dimer−monomer dissociation of A4V and WT SOD, samples were analyzed on Superdex 75 (3.2/30) gel-filtration column (Pharmacia).

*Characterization of Oligomeric A4V by Electron Microscopy*. Purified A4V fractions were diluted 6-fold with TBS prior to adsorption to glow-discharged, carbon-coated copper grids. Grids were washed with four drops of buffer and stained with two drops of freshly prepared 0.75% (w/v) uranyl formate (Pfaltz & Bauer, Waterbury, CT 06708). Specimens were inspected with a Philips Tecnai 12 electron microscope operated at 120 kV, and images were taken at a nominal magnification of 52 000 using low-dose procedures. For image processing, 31 images of A4V (late fraction and void peak) and 51 images of A4V (middle fraction and dimer peak) were digitized with a Zeiss SCAI scanner using a pixel size of 4.04 Å at the specimen level. From the digitized images, 5815 (A4V) particles were selected for further

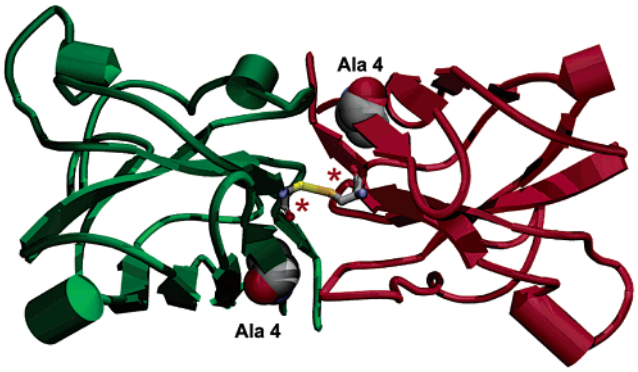


FIGURE 3: Ribbon diagram of WT with the engineered disulfide bridge (its conformation is optimized) between residues C148 and C148′ of opposite subunits. The red ∗ indicate the position of the residue that was changed to cysteine to make the disulfide bridge. Alanine 4 is shown in space-filling mode (carbon is gray; carbonyl oxygen is red).

computational processing using the SPIDER image-processing package. The 5000−6000 particle images were subjected to 10 rounds of alignment and classification specifying 100 output classes.

## RESULTS

*The A4V Mutation Promotes Aggregation of SOD1*. Alanine 4 is located at the SOD1 dimer interface (Figure 3) (*29*), which suggests that the A4V dimer could be destabilized relative to the WT dimer. Not surprisingly, A4V differed significantly from WT (*12*, *18*, *30*). First, consistent with the observations of Hayward et al. (*12*), A4V had a significantly lower copper content (ca. 50% of WT) than WT (UV−visible spectrum, 680/278 nm). Second, A4V was more prone to aggregate than WT: when incubated at 100 $\mu$M at 37 °C, WT was stable for days, whereas A4V dimer began to disappear within 1 h (Figure 1a). Concurrent with dimer disappearance, a heterogeneous population of A4V aggregates appeared.

*A4V Oligomers Include Pore-like and Large Spherical Structures.* The heterogeneous population of A4V aggregates was fractionated using Superdex 200 size-exclusion chromatography (indicated in Figure 1a), and the fractions were analyzed by electron microscopy (Figure 1b). The fraction of highest molecular weight (F1) contained large (diameter of ca. 50 nm) sphere-like and irregular oligomeric structures (Figure 1b). Smaller structures, including pore-like structures that resembled "amyloid pores" formed by α-synuclein or $\beta$-amyloid protein (*31*), were found in fractions of lower molecular weight (F2 and F3, see red arrows). No fibrillar structures were produced under these conditions (or any others that were tested). Images of the fraction containing the A4V dimer (F4) revealed structures consistent with the WT dimer structure in the crystalline state (diameter of ca. 7 nm). To improve resolution, similar structures were grouped, and images were averaged. Three distinct morphologies were observed: the A4V dimer (Figure 1c, top panels), A4V pore-like oligomers comprising different numbers of distinct subunits (each "subunit" may be an A4V dimer or monomer) and with diameters of 7−20 nm, (middle panels), and large spherical structures (bottom panels). Close examination of the latter structures suggests that they may be products of pore aggregation.

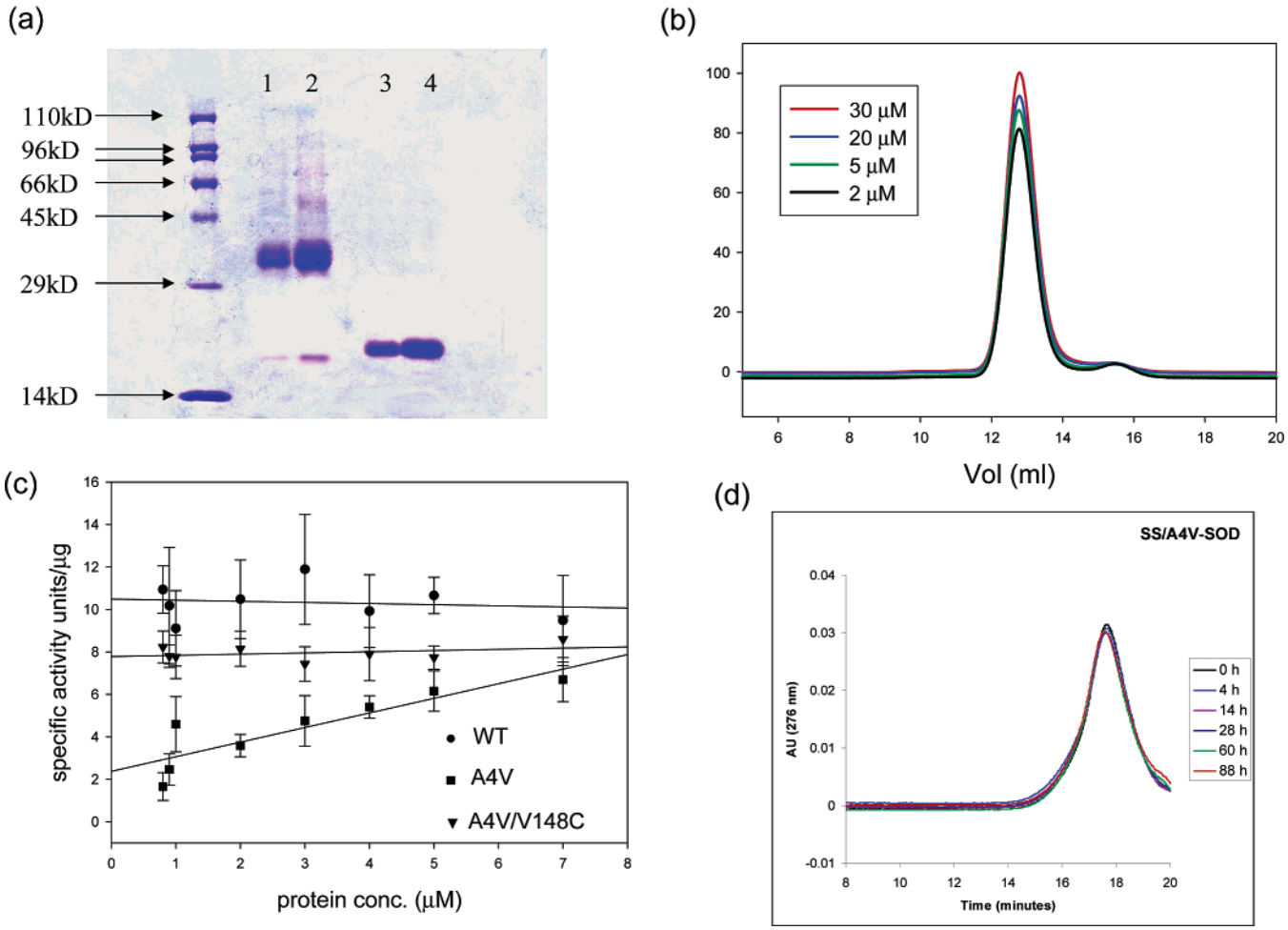


FIGURE 4: (a) SDS−PAGE analysis of the engineered mutants. Lanes 1 and 2 are V148C and A4V/V148C, respectively, analyzed under nonreducing conditions. These proteins migrate as ~32 kDa on SDS−PAGE indicating the presence of an intersubunit disulfide. Lanes 3 and 4 are V148C and A4V/V148C analyzed under reducing conditions. Protein samples for analysis under reducing conditions were boiled for 10 min with SDS−PAGE loading buffer (5% SDS, 0.1 M Tris, pH 8.8, 20% glycerol, and 25 mM DTT), and samples for nonreducing conditions were boiled with SDS−PAGE loading buffer without DTT (5% SDS, 0.1 M Tris, pH 8.8, and 20% glycerol) for the same time period. (b) Size-exclusion chromatography (Superdex 75) profile for $(A4V/V148C)_2$ under conditions described in Figure 2 legend. (c) Specific activity of WT (●), A4V (■), and $(A4V/V148C)_2$ (▼) as a function of protein concentration using a coupled enzyme assay with xanthine oxidase (see Materials and Methods section for details). (d) Size-exclusion chromatography of $(A4V/V148C)_2$ under conditions described in Figure 1a legend. $(A4V/V148C)_2$ does not aggregate under these conditions (nor does V148C).

*At Lower Concentrations, Where Aggregation Is Extremely Slow, A4V Exists as a Mixture of Dimer and Monomer, While WT Is Purely Dimeric.* To determine whether the A4V mutation destabilized the dimeric enzyme, A4V and WT (1−30 $\mu$M) were analyzed by size-exclusion chromatography (Superdex 75) (Figure 2). WT dimer was stable over this concentration range (Figure 2b). In contrast, the A4V dimer population decreased at low concentration ([A4V] < 20 $\mu$M) and a species of lower molecular weight appeared (Figure 2b). Multiangle light scattering indicated that the molecular mass of this species was ca. 16 kD, consistent with the mass of A4V monomer (not shown). The A4V-derived ~16 kD species was populated in a concentration-dependent manner (Figure 2b), such that it was the predominant species at 2 $\mu$M. The approximate dissociation constant for A4V was 3 $\mu$M. The fact that A4V caused dimer destabilization and aggregation suggested that dissociation of the A4V dimer may be *required* for aggregation to occur. To test this possibility, we engineered a covalent dimeric form of A4V that was incapable of dissociation.

*Introduction of an Intersubunit Disulfide Bond into A4V To Produce $(A4V/V148C)_2$ Prevented Monomerization.* Stabilization of the A4V dimer was attempted by insertion of an intersubunit disulfide bond. Since the mere proximity of cysteine residues is not sufficient to guarantee formation of a disulfide bond (*32*, *33*) (geometric constraints are also important), we utilized the program MODIP (gift from Dr. R. Sowdhamini, NCBS, TIFR) (*34*) to predict stereochemically suitable sites for mutagenesis and insertion of an unstrained disulfide bond. The coordinates of WT (pdb code; 1spd.pdb) were used for our calculations, since the A4V dimer structure has not been determined. Valine 148 was chosen for mutagenesis since the resultant C148−C148′ disulfide bond was predicted to be virtually strain-free (Figure 3). The double mutant A4V/V148C was purified and analyzed by SDS−PAGE under *nonreducing* conditions was found to migrate at ~32 kDa, confirming that the intermolecular disulfide bond had indeed formed (Figure 4a). Like WT (and unlike A4V), the A4V/V148C dimer, $(A4V/V148C)_2$, was stable over the concentration of range of 30−1

$\mu$M (Figure 4b). As a control, the V148C mutation was made in the WT background. V148C was dimeric ($(V148C)_2$) by SDS−PAGE and gel filtration (not shown).

*$(A4V/V148C)_2$ and WT Had Comparable Specific Activity at Concentrations Where A4V Activity Was Reduced.* To test whether disulfide bond formation altered the enzymatic activity of A4V, we determined the specific activity of WT, A4V, and $(A4V/V148C)_2$ over a range of concentrations. The specific activity of WT (ca. 10000 U/mg) was independent of concentration between 1 and 10 $\mu$M (Figure 4c). At concentrations below 4 $\mu$M, A4V had a lower specific activity than WT, confirming published observations (*12*). However, A4V activity was concentration-dependent, consistent with the notion that the monomeric species has reduced activity due to minor changes near the active site of SOD (*35*). The double mutant $(A4V/V148C)_2$ had greater catalytic activity than A4V at low concentrations (Figure 4c), and like WT, the specific activity was concentration-independent, consistent with the proposal that the intersubunit disulfide bond had stabilized a WT-like dimeric structure. The copper content of $(A4V/V148C)_2$ was ca. 75% that of WT (150% of A4V). The control protein $(V148C)_2$ had comparable specific activity to WT (not shown).

*$(A4V/V148C)_2$, Unlike A4V, Did Not Aggregate.* $(A4V/V148C)_2$ was incubated under conditions where A4V aggregated but WT did not (37 °C, see above and Figure 1). $(A4V/V148C)_2$ was stable over an 80 h period (A4V began to aggregate within 1 h) (Figure 4d). In fact, no aggregation was observed after 170 h at 42 °C (not shown). Like $(A4V/V148C)_2$ and WT, $(V148C)_2$ did not aggregate (not shown).

## DISCUSSION

We demonstrate here that A4V, a protein linked to the most aggressive form of FALS, has an increased propensity (relative to WT) to monomerize, to aggregate, and to form amyloid pores. The pore-like A4V aggregates, which resemble those formed in vitro from A4V and WT (*36*), also resemble amyloid pores comprising disease-linked mutant forms of α-synuclein (familial Parkinson's disease) and $\beta$-amyloid protein (familial Alzheimer's disease) (*16*). Similar pore-like structures comprising WT, A4V, and two other FALS-linked mutants, G85R and G37R, have been reported (*36*). Hart et al. have reported annular forms of G85R and G37R in crystals (*37, 38*). These structures do not involve rearrangements at the dimer interface, so they are not likely to be identical to the A4V pores shown here (see below), though they may have some features in common. Several potential targets for the A4V amyloid pore can be envisioned, including the mitochondrial membranes, which are compromised in ALS motor neurons (*39*). Of course, A4V aggregates may have additional pathogenic effects that do not depend on pore formation, such as toxin-generating abnormal enzymatic activity (*30*).

The behavior of the engineered disulfide-stabilized dimer $(A4V/V148C)_2$ suggests that dimer dissociation and aggregation are necessarily linked. The fact that SOD dimer dissociates to yield monomers has been observed previously for SOD purified from other species (*40*−*43*). The dissociation of multimeric proteins often leads to unfolding and aggregation (*44*−*50*), and these processes can be promoted by disease-associated mutations (*44, 48, 51*−*53*). The best-characterized example of such a system is the protein transthyretin (TTR), product of a gene linked to familial amyloid polyneuropathy (FAP) (*54, 55*). Many FAP mutations (which in the case of FALS, they are predominantly autosomal dominant, gain of function mutations) destabilize the native TTR tetramer, facilitating its dissociation, unfolding, and aggregation (*56*−*60*). Stabilization of the TTR tetramer by interaction with analogues of its natural ligand, thyroxine, prevents its in vitro aggregation (*57, 58*). Whether these block pathogenesis in vivo is under investigation.

We have not yet determined whether some or all of the less common FALS-linked SOD1 mutations also result in population of an aggregation-prone monomer. Some of these mutations have been demonstrated to affect [1] substrate binding, [2] copper binding at the active site, [3] thermodynamic or kinetic stability of the protein or both, [4] zinc binding, and [5] intersubunit interactions (*12, 19, 61, 62*). It is likely that all of these changes are linked to increased population of the aggregation-prone, partially unfolded monomer. Metal binding and dimer stability appear to be linked. Thus destabilization of the dimer interface by A4V affects copper binding, despite the fact that the mutation is located far from the copper binding site (*12, 19, 62*). Conversely, removal of metal affects dimer stability and aggregation: treatment of A4V with EDTA greatly destabilizes the dimer and accelerates aggregation (S.R. and P.L., unpublished results). EDTA treatment promotes in vitro aggregation of other FALS-associated mutants including G93A, G85R, H46R, and S134N, as well as WT (S.R. and P.L., unpublished results).

Engineering of disulfide bridges to stabilize protein structures and prevent in vitro unfolding and aggregation is effective in the case of A4V/V148C, as well as other cases (*49, 50, 63*−*69*). However, the greatest potential value of this approach is that it allows the link between SOD1 aggregation and FALS pathogenesis to be tested in vivo. The V148C−V148C′ disulfide bridge, provided that it forms in vivo, should prevent aggregation and, if aggregation is pathogenic, disease onset in mouse models of FALS (*70*). Demonstration of this effect would validate an extensive search for drug-like molecules that had a similar dimer-stabilizing effect, analogous to those described in the case of TTR (*57, 58*). Such molecules could be developed into desperately needed therapeutics for FALS.

## ACKNOWLEDGMENT

We acknowledge discussions with Tomas Ding (Center for Neurologic Diseases) who has obtained atomic force microscopic images (to be published elsewhere) that indicate pore-like A4V aggregates. We also thank Prof. C. Ramakrishnan (IISc, India) and R. Sowdhamini (NCBS, India) for their help with the disulfide modeling program MODIP.

## REFERENCES

1. Xiong, Z. Q., and McNamara, J. O. (2002) Fas(t) balls and Lou Gehrig disease. A clue to selective vulnerability of motor neurons? *Neuron 35*, 1011−1013.
2. Cleveland, D. W., and Rothstein, J. D. (2001) From Charcot to Lou Gehrig: deciphering selective motor neuron death in ALS, *Nat. Rev. Neurosci. 2*, 806−819.
3. Brown, R. H., Jr. (1995) Superoxide dismutase in familial amyotrophic lateral sclerosis: models for gain of function, *Curr. Opin. Neurobiol. 5*, 841−846.

4. Brown, R. H. (1994) A transgenic-mouse model of amyotrophic lateral sclerosis, *N. Engl. J. Med. 331*, 1091−1092.
5. Cleveland, D. W., Laing, N., Hurse, P. V., and Brown, R. H., Jr. (1995) Toxic mutants in Charcot's sclerosis, *Nature 378*, 342−343.
6. Brown, R. H., Jr., and Robberecht, W. (2001) Amyotrophic lateral sclerosis: pathogenesis, *Semin. Neurol. 21*, 131−139.
7. Bruijn, L. I., Houseweart, M. K., Kato, S., Anderson, K. L., Anderson, S. D., Ohama, E., Reaume, A. G., Scott, R. W., and Cleveland, D. W. (1998) Aggregation and motor neuron toxicity of an ALS-linked SOD1 mutant independent from wild-type SOD1, *Science 281*, 1851−1854.
8. Bowling, A. C., Schulz, J. B., Brown, R. H., Jr., and Beal, M. F. (1993) Superoxide dismutase activity, oxidative damage, and mitochondrial energy metabolism in familial and sporadic amyotrophic lateral sclerosis, *J. Neurochem. 61*, 2322−2325.
9. Borchelt, D. R., Lee, M. K., Slunt, H. S., Guarnieri, M., Xu, Z. S., Wong, P. C., Brown, R. H., Jr., Price, D. L., Sisodia, S. S., and Cleveland, D. W. (1994) Superoxide dismutase 1 with mutations linked to familial amyotrophic lateral sclerosis possesses significant activity, *Proc. Natl. Acad. Sci. U.S.A. 91*, 8292−8296.
10. Rothstein, J. D., Bristol, L. A., Hosler, B., Brown, R. H., Jr., and Kuncl, R. W. (1994) Chronic inhibition of superoxide dismutase produces apoptotic death of spinal neurons, *Proc. Natl. Acad. Sci. U.S.A. 91*, 4155−4159.
11. Lindberg, M. J., Tibell, L., and Oliveberg, M. (2002) Common denominator of Cu/Zn superoxide dismutase mutants associated with amyotrophic lateral sclerosis: decreased stability of the apo state, *Proc. Natl. Acad. Sci. U.S.A. 99*, 16607−16612.
12. Hayward, L. J., Rodriguez, J. A., Kim, J. W., Tiwari, A., Goto, J. J., Cabelli, D. E., Valentine, J. S., and Brown, R. H., Jr. (2002) Decreased metallation and activity in subsets of mutant superoxide dismutases associated with familial amyotrophic lateral sclerosis, *J. Biol. Chem. 277*, 15923−15931.
13. Nakano, R., Inuzuka, T., Kikugawa, K., Takahashi, H., Sakimura, K., Fujii, J., Taniguchi, N., and Tsuji, S. (1996) Instability of mutant Cu/Zn superoxide dismutase (Ala4Thr) associated with familial amyotrophic lateral sclerosis, *Neurosci. Lett. 211*, 129−131.
14. Deng, H. X., Hentati, A., Tainer, J. A., Iqbal, Z., Cayabyab, A., Hung, W. Y., Getzoff, E. D., Hu, P., Herzfeldt, B., Rood, R. P., Warner, C., Deng, G., Soriano, E., Smyth, C., Parge, H. E., Ahmed, A., Roses, A. D., Hallewell, R. A., Perciak-Vance, M. A., and Siddique, T. (1993) Amyotrophic lateral sclerosis and structural defects in Cu,Zn superoxide dismutase, *Science 261*, 1047−1051.
15. Julien, J. P. (2001) Amyotrophic lateral sclerosis. Unfolding the toxicity of the misfolded, *Cell 104*, 581−591.
16. Lashuel, H. A., Hartley, D., Petre, B. M., Walz, T., and Lansbury, P. T., Jr. (2002) Neurodegenerative disease: amyloid pores from pathogenic mutations, *Nature 418*, 291.
17. Assfalg, M., Banci, L., Bertini, I., Turano, P., and Vasos, P. R. (2003) Superoxide dismutase folding/unfolding pathway: role of the metal ions in modulating structural and dynamical features, *J. Mol. Biol. 330*, 145−158.
18. Stathopulos, P. B., Rumfeldt, J. A., Scholz, G. A., Irani, R. A., Frey, H. E., Hallewell, R. A., Lepock, J. R., and Meiering, E. M. (2003) Cu/Zn superoxide dismutase mutants associated with amyotrophic lateral sclerosis show enhanced formation of aggregates in vitro, *Proc. Natl. Acad. Sci. U.S.A. 100*, 7021−7026.
19. Cardoso, R. M., Thayer, M. M., DiDonato, M., Lo, T. P., Bruns, C. K., Getzoff, E. D., and Tainer, J. A. (2002) Insights into Lou Gehrig's disease from the structure and instability of the A4V mutant of human Cu,Zn superoxide dismutase, *J. Mol. Biol. 324*, 247−256.
20. Ogawa, Y., Kosaka, H., Nakanishi, T., Shimizu, A., Ohoi, N., Shouji, H., Yanagihara, T., and Sakoda, S. (1997) Stability of mutant superoxide dismutase-1 associated with familial amyotrophic lateral sclerosis determines the manner of copper release and induction of thioredoxin in erythrocytes, *Biochem. Biophys. Res. Commun. 241*, 251−257.
21. Watanabe, Y., Kono, Y., Nanba, E., Ohama, E., and Nakashima, K. (1997) Instability of expressed Cu/Zn superoxide dismutase with 2 bp deletion found in familial amyotrophic lateral sclerosis, *FEBS Lett. 400*, 108−112.
22. Banci, L., Bertini, I., Cabelli, D. E., Hallewell, R. A., Luchinat, C., and Viezzoli, M. S. (1991) Advances in the understanding of the structure−function relationship in Cu,Zn superoxide dismutase, *Free Radical Res. Commun. 12−13* (Part 1), 239−251.
23. McRee, D. E., Redford, S. M., Getzoff, E. D., Lepock, J. R., Hallewell, R. A., and Tainer, J. A. (1990) Changes in crystallographic structure and thermostability of a Cu,Zn superoxide dismutase mutant resulting from the removal of a buried cysteine, *J. Biol. Chem. 265*, 14234−14241.
24. Potter, S. Z., and Valentine, J. S. (2003) The perplexing role of copper−zinc superoxide dismutase in amyotrophic lateral sclerosis (Lou Gehrig's disease), *J. Biol. Inorg. Chem. 8*, 373−380.
25. Rabizadeh, S., Gralla, E. B., Borchelt, D. R., Gwinn, R., Valentine, J. S., Sisodia, S., Wong, P., Lee, M., Hahn, H., and Bredesen, D. E. (1995) Mutations associated with amyotrophic lateral sclerosis convert superoxide dismutase from an antiapoptotic gene to a proapoptotic gene: studies in yeast and neural cells, *Proc. Natl. Acad. Sci. U.S.A. 92*, 3024−3028.
26. Nishida, C. R., Gralla, E. B., and Valentine, J. S. (1994) Characterization of three yeast copper−zinc superoxide dismutase mutants analogous to those coded for in familial amyotrophic lateral sclerosis, *Proc. Natl. Acad. Sci. U.S.A. 91*, 9906−9910.
27. Juneja, T., Pericak-Vance, M. A., Laing, N. G., Dave, S., and Siddique, T. (1997) Prognosis in familial amyotrophic lateral sclerosis: progression and survival in patients with glu100gly and ala4val mutations in Cu,Zn superoxide dismutase, *Neurology 48*, 55−57.
28. Okado-Matsumoto, A., and Fridovich, I. (2001) Assay of superoxide dismutase: cautions relevant to the use of cytochrome *c*, a sulfonated tetrazolium, and cyanide, *Anal. Biochem. 298*, 337−342.
29. Roberts, V. A., Fisher, C. L., Redford, S. M., McRee, D. E., Parge, H. E., Getzoff, E. D., and Tainer, J. A. (1991) Mechanism and atomic structure of superoxide dismutase, *Free Radical Res. Commun. 12−13* (Part 1), 269−278.
30. Yim, H. S., Kang, J. H., Chock, P. B., Stadtman, E. R., and Yim, M. B. (1997) A familial amyotrophic lateral sclerosis-associated A4V Cu, Zn-superoxide dismutase mutant has a lower Km for hydrogen peroxide. Correlation between clinical severity and the Km value, *J. Biol. Chem. 272*, 8861−8863.
31. Lashuel, H. A., Petre, B. M., Wall, J., Simon, M., Nowak, R. J., Walz, T., and Lansbury, P. T., Jr. (2002) Alpha-synuclein, especially the Parkinson's disease-associated mutants, forms pore-like annular and tubular protofibrils, *J. Mol. Biol. 322*, 1089−1102.
32. Srinivasan, N., Sowdhamini, R., Ramakrishnan, C., and Balaram, P. (1990) Conformations of disulfide bridges in proteins, *Int. J. Pept. Protein Res. 36*, 147−155.
33. Sowdhamini, R., Srinivasan, N., Shoichet, B., Santi, D. V., Ramakrishnan, C., and Balaram, P. (1989) Stereochemical modeling of disulfide bridges. Criteria for introduction into proteins by site-directed mutagenesis, *Protein Eng. 3*, 95−103.
34. Sowdhamini, R., Ramakrishnan, C., and Balaram, P. (1993) Modelling multiple disulphide loop containing polypeptides by random conformation generation. The test cases of alpha-conotoxin GI and endothelin I, *Protein Eng. 6*, 873−882.
35. Banci, L., Bertini, I., Bruni, B., Carloni, P., Luchinat, C., Mangani, S., Orioli, P. L., Piccioli, M., Ripniewski, W., and Wilson, K. S. (1994) X-ray, NMR and molecular dynamics studies on reduced bovine superoxide dismutase: implications for the mechanism, *Biochem. Biophys. Res. Commun. 202*, 1088−1095.
36. Chung, J., Yang, H., de Beus, M. D., Ryu, C. Y., Cho, K., and Colon, W. (2003) Cu/Zn superoxide dismutase can form pore-like structures, *Biochem. Biophys. Res. Commun. 312*, 873−876.
37. Elam, J. S., Malek, K., Rodriguez, J. A., Doucette, P. A., Taylor, A. B., Hayward, L. J., Cabelli, D. E., Valentine, J. S., and Hart, P. J. (2003) An alternative mechanism of bicarbonate-mediated peroxidation by copper−zinc superoxide dismutase: rates enhanced via proposed enzyme-associated peroxycarbonate intermediate, *J. Biol. Chem. 278*, 21032−21039.
38. Elam, J. S., Taylor, A. B., Strange, R., Antonyuk, S., Doucette, P. A., Rodriguez, J. A., Hasnain, S. S., Hayward, L. J., Valentine, J. S., Yeates, T. O., and Hart, P. J. (2003) Amyloid-like filaments and water-filled nanotubes formed by SOD1 mutant proteins linked to familial ALS, *Nat. Struct. Biol. 10*, 461−467.
39. Higgins, C. M., Jung, C., Ding, H., and Xu, Z. (2002) Mutant Cu, Zn superoxide dismutase that causes motoneuron degeneration is present in mitochondria in the CNS, *J. Neurosci. 22*, No. RC215.
40. Cioni, P., Stroppolo, M. E., Desideri, A., and Strambini, G. B. (2001) Dynamic features of the subunit interface of Cu,Zn superoxide dismutase as probed by tryptophan phosphorescence, *Arch. Biochem. Biophys. 391*, 111−118.

41. D'Orazio, M., Battistoni, A., Stroppolo, M. E., and Desideri, A. (2000) Single mutation induces a metal-dependent subunit association in dimeric Cu,Zn superoxide dismutase, *Biochem. Biophys. Res. Commun. 272*, 81−83.
42. Stroppolo, M. E., Nuzzo, S., Pesce, A., Rosano, C., Battistoni, A., Bolognesi, M., Mobilio, S., and Desideri, A. (1998) On the coordination and oxidation states of the active-site copper ion in prokaryotic Cu,Zn superoxide dismutases, *Biochem. Biophys. Res. Commun. 249*, 579−582.
43. Stroppolo, M. E., Malvezzi-Campeggi, F., Mei, G., Rosato, N., and Desideri, A. (2000) Role of the tertiary and quaternary structures in the stability of dimeric copper, zinc superoxide dismutases, *Arch. Biochem. Biophys. 377*, 215−218.
44. McGovern, P., Reisberg, P., and Olson, J. S. (1976) Aggregation of deoxyhemoglobin subunits, *J. Biol. Chem. 251*, 7871−7879.
45. Konno, H., Yamamoto, T., Iwasaki, Y., and Iizuka, H. (1986) Shy-Drager syndrome and amyotrophic lateral sclerosis. Cytoarchitectonic and morphometric studies of sacral autonomic neurons, *J. Neurol. Sci. 73*, 193−204.
46. Hargrove, M. S., Whitaker, T., Olson, J. S., Vali, R. J., and Mathews, A. J. (1997) Quaternary structure regulates hemin dissociation from human hemoglobin, *J. Biol. Chem. 272*, 17385−17389.
47. Bras, G. L., Teschner, W., Deville-Bonne, D., and Garel, J. R. (1989) Urea-induced inactivation, dissociation, and unfolding of the allosteric phosphofructokinase from *Escherichia coli*, *Biochemistry 28*, 6836−6841.
48. Barry, J. K., and Matthews, K. S. (1999) Thermodynamic analysis of unfolding and dissociation in lactose repressor protein, *Biochemistry 38*, 6520−6528.
49. Agarwalla, S., Gokhale, R. S., Santi, D. V., and Balaram, P. (1996) Covalent tethering of the dimer interface annuls aggregation in thymidylate synthase, *Protein Sci. 5*, 270−277.
50. Gokhale, R. S., Agarwalla, S., Santi, D. V., and Balaram, P. (1996) Covalent reinforcement of a fragile region in the dimeric enzyme thymidylate synthase stabilizes the protein against chaotrope-induced unfolding, *Biochemistry 35*, 7150−7158.
51. Banci, L., Bertini, I., Cantini, F., D'Onofrio, M., and Viezzoli, M. S. (2002) Structure and dynamics of copper-free SOD: The protein before binding copper, *Protein Sci. 11*, 2479−2492.
52. Banci, L., Bertini, I., Cramaro, F., Del Conte, R., and Viezzoli, M. S. (2002) The solution structure of reduced dimeric copper zinc superoxide dismutase. The structural effects of dimerization, *Eur. J. Biochem. 269*, 1905−1915.
53. Finke, J. M., Gross, L. A., Ho, H. M., Sept, D., Zimm, B. H., and Jennings, P. A. (2000) Commitment to folded and aggregated states occurs late in interleukin-1 beta folding, *Biochemistry 39*, 15633−15642.
54. Kelly, J. W. (1997) Amyloid fibril formation and protein misassembly: a structural quest for insights into amyloid and prion diseases, *Structure 5*, 595−600.
55. Kelly, J. W., Colon, W., Lai, Z., Lashuel, H. A., McCulloch, J., McCutchen, S. L., Miroy, G. J., and Peterson, S. A. (1997) Transthyretin quaternary and tertiary structural changes facilitate misassembly into amyloid, *Adv. Protein Chem. 50*, 161−181.
56. Schneider, F., Hammarstrom, P., and Kelly, J. W. (2001) Transthyretin slowly exchanges subunits under physiological conditions: A convenient chromatographic method to study subunit exchange in oligomeric proteins, *Protein Sci. 10*, 1606−1613.
57. Baures, P. W., Peterson, S. A., and Kelly, J. W. (1998) Discovering transthyretin amyloid fibril inhibitors by limited screening, *Bioorg. Med. Chem. 6*, 1389−1401.
58. Miroy, G. J., Lai, Z., Lashuel, H. A., Peterson, S. A., Strang, C., and Kelly, J. W. (1996) Inhibiting transthyretin amyloid fibril formation via protein stabilization, *Proc. Natl. Acad. Sci. U.S.A. 93*, 15051−15056.
59. Hammarstrom, P., Jiang, X., Deechongkit, S., and Kelly, J. W. (2001) Anion shielding of electrostatic repulsions in transthyretin modulates stability and amyloidosis: insight into the chaotrope unfolding dichotomy, *Biochemistry 40*, 11453−11459.
60. Hammarstrom, P., Schneider, F., and Kelly, J. W. (2001) Trans-suppression of misfolding in an amyloid disease, *Science 293*, 2459−2462.
61. Watanabe, M., Dykes-Hoberg, M., Culotta, V. C., Price, D. L., Wong, P. C., and Rothstein, J. D. (2001) Histological evidence of protein aggregation in mutant SOD1 transgenic mice and in amyotrophic lateral sclerosis neural tissues, *Neurobiol. Dis. 8*, 933−941.
62. DiDonato, M., Craig, L., Huff, M. E., Thayer, M. M., Cardoso, R. M., Kassmann, C. J., Lo, T. P., Bruns, C. K., Powers, E. T., Kelly, J. W., Getzoff, E. D., and Tainer, J. A. (2003) ALS mutants of human superoxide dismutase form fibrous aggregates via framework destabilization, *J. Mol. Biol. 332*, 601−615.
63. Gokhale, R. S., Ray, S. S., Balaram, H., and Balaram, P. (1999) Unfolding of *Plasmodium falciparum* triosephosphate isomerase in urea and guanidinium chloride: evidence for a novel disulfide exchange reaction in a covalently cross-linked mutant, *Biochemistry 38*, 423−431.
64. Gopal, B., Ray, S. S., Gokhale, R. S., Balaram, H., Murthy, M. R., and Balaram, P. (1999) Cavity-creating mutation at the dimer interface of *Plasmodium falciparum* triosephosphate isomerase: restoration of stability by disulfide cross-linking of subunits, *Biochemistry 38*, 478−486.
65. Velanker, S. S., Gokhale, R. S., Ray, S. S., Gopal, B., Parthasarathy, S., Santi, D. V., Balaram, P., and Murthy, M. R. (1999) Disulfide engineering at the dimer interface of *Lactobacillus casei* thymidylate synthase: crystal structure of the T155C/E188C/C244T mutant, *Protein Sci. 8*, 930−933.
66. Gokhale, R. S., Agarwalla, S., Francis, V. S., Santi, D. V., and Balaram, P. (1994) Thermal stabilization of thymidylate synthase by engineering two disulfide bridges across the dimer interface, *J. Mol. Biol. 235*, 89−94.
67. Jacobson, R. H., Matsumura, M., Faber, H. R., and Matthews, B. W. (1992) Structure of a stabilizing disulfide bridge mutant that closes the active-site cleft of T4 lysozyme, *Protein Sci. 1*, 46−57.
68. Pjura, P. E., Matsumura, M., Wozniak, J. A., and Matthews, B. W. (1990) Structure of a thermostable disulfide-bridge mutant of phage T4 lysozyme shows that an engineered cross-link in a flexible region does not increase the rigidity of the folded protein, *Biochemistry 29*, 2592−2598.
69. Matsumura, M., and Matthews, B. W. (1991) Stabilization of functional proteins by introduction of multiple disulfide bonds, *Methods Enzymol. 202*, 336−356.
70. Kunst, C. B., Mezey, E., Brownstein, M. J., and Patterson, D. (1997) Mutations in SOD1 associated with amyotrophic lateral sclerosis cause novel protein interactions, *Nat. Genet. 15*, 91−94.

BI030246R